Atomosphere boundary layer height determination and observation from ceilometer measurements over Hefei during the total solar on July 22, 2009 eclipse

Junfeng He (何俊峰)[1,2*], Wenqing Liu (刘文清)[1], Yunjun Zhang (张玉钧)[1], Ruifeng Kan (阚瑞峰)[1], Zhenyi Chen (陈臻懿)[1], and Jun Ruan (阮 俊)[1]

[1] *Anhui Institute of Optics and Fine Mechanics, Chinese Academy of Sciences, Hefei 230031, China*

[2] *Artillery Academy, Hefei 230031, China*

[*] *E-mail: hejunfeng@aiofm.ac.cn*

Received December 4, 2009

Using an improved inflexion point method (IIPM), we investigate atmosphere boundary layer (ABL) height evolution over Hefei during the total solar eclipse on July 22, 2009. A lidar ceilometer is used in ground-based observations. Estimations of ABL heights before, during, and after the solar eclipse are analyzed using the IIPM. Results indicate that the IIPM, which is less sensitive to background noise, is more suitable in detecting ABL height and temporal evolution. Data demonstrate that the total solar eclipse resultes in a decrease in ABL height, indicating a suppression of turbulence activity, similar to that observed during the sunset hours. Changes in ABL height are associated with a slow change in temperature, indicating a significant weakening of penetrative convection and a time lag between ABL response and the reduction in solar radiation.

OCIS codes: 010.0010, 140.0140, 280.0280, 290.0290.

doi: 10.3788/COL20100805.0439.

On July 22, 2009, a solar eclipse covering the Yangzi River Zone, China, took place. The total eclipse lasted for more than 6 min, the longest total eclipse to be observed in China from 1814 to 2309. Hefei is located in the central part of China (latitude 32 °, longitude 117 °), right within the total eclipse zone. A solar eclipse can simply be considered as a fast sunset and sunrise. As an astronomical event, it provides a unique opportunity to study various atmospheric phenomena, especially as incoming solar radiation is sharply turned off and on during such events. A solar eclipse provides natural experimental conditions in studying the atmosphere's responses to solar radiation changes because of the sudden reduction in solar radiation. The atmosphere boundary layer (ABL) is part of the convective layer, which is directly affected by the Earth's surface. It is where the transport of mass, energy, and momentum towards other parts of the atmosphere takes place through a turbulence process. A change in radiative heating or cooling is first felt in the ABL before it is felt by the free atmosphere. The ABL height has a strong impact on local and regional weather, as well as on air quality. Regarding air quality, ABL height determines the volume available for pollutant dispersion, including the resulting concentrations. It is therefore one of the fundamental parameters in many dispersion models. Continuous observations of the ABL top with high vertical and temporal resolutions are thus desirable to support weather and air quality predictions.

ABL responds to surface forcing by frictional drag, evaporation and transpiration, and sensible heat transfer with a timescale of an hour or less[1]. The ABL has a clearly outlined structure that differs from daytime to nighttime. During a normal day, a convective atmospheric boundary layer (CABL) develops, reaching a quasi-steady state in the afternoon. The CABL has a mixed layer from the ground up to the interfacial layer with the free atmosphere, where strong thermal inversion transpires. The ABL afternoon/evening transition is marked before sunset by the development of a surface inversion related to surface cooling. The CABL, called the residual layer after sunset, becomes neutral above that stable layer. After sunrise, the stable layer is destroyed and a new mixing layer (ML) develops. During a solar eclipse, the two transition situations are reproduced, with much shorter time scales than those in the normal diurnal cycle, providing an excellent chance to investigate the mechanisms that drive the evolution of ABL.

Research on ABL evolution during a normal day has been extensively conducted using various complex instruments. There have been several important findings related to ABL evolution during a solar eclipse. Antonia *et al.* found that the surface layer turbulence follows a continuum of equilibrium states in response to stability changes brought about by changes in surface heat flux during the solar eclipse on October 23, 1976, over Delinquin, Australia. With a lidar, Amiridis *et al.* studied the dynamics of ABL during the solar eclipse on August 11, 1999, over Bulgaria and found that the solar eclipse affected the atmosphere's meteorological parameters, ozone concentration, and mixing layer height[2].

The aim of this work is to study the height response of ABL to the July 2009 solar eclipse by observing the range-squared-corrected backscatter signal (RSCS) of the atmosphere using a lidar ceilometer. An improved inflexion point method (IIPM) is proposed to analyze backscatter data and to identify ABL height.

Using the modern ground-based remote sensing techniques to monitor diurnal variations of atmospheric lay-

ering and ABL seems promising. In active remote sensors such as 1idars, aerosols are used as tracers of the ABL. The ABL is typically moister and has high aerosol concentration, thus scattering more laser light than the free troposphere. Lidar can easily detect the boundary between the two layers. Its long distance ranging capability, high resolution, and high repetition rate make it one of the most suitable techniques in analyzing ABL structure and in determining ABL height and entrainment zone thickness[1,3−7].

In recent years, the application of optical remote sensing in the study of ABL has been focused on the use of a lidar ceilometer, which can be regarded as a small, simple lidar. The ceilometer Vaisala CL31 used in this study mainly consists of three parts: the laser transmitter unit, the signal reception and detection unit, and the data acquisition and control unit. Figure 1 and Table 1 show the schematic structure of the system and the primary technical parameters, respectively. The single-lens ceilometer used in this experiment measures the optical backscatter intensity of the atmosphere at a wavelength of 905 nm. The laser diodes used in this ceilometer work with pulsed mode at a repetition rate of 10 kHz. The ceilometer samples the return signal every 66.7 ns from 0 to 50 μs, providing a spatial resolution of 10 m from the ground up to an altitude of 7.5 km. The intensity of the backscatter signal mainly depends on particulate concentration in the atmosphere. The size of particles varies with moisture content; hence, reflectivity is also influenced by atmospheric humidity. Clouds, fog, and precipitation inhibit the measurements. The performance of the ceilometer has many advantages in analyzing boundary layer structures. Compared with more sophisticated lidar systems, ceilometers have a low first range gate and involve eye-safe operations. Moreover, it is maintenance-free, low-cost, and portable. The major disadvantage of using a ceilometer is its short accessible range (mostly below 10 km) because of low power emitted from laser diodes. However, in ABL (mostly below 3 km) studies, this does not present a problem.

Using aerosol particles as tracers, the top of the ML, which is the height where the lidar signal profile exhibits a discontinuity between the ML and the free troposphere, can be determined. In this letter, the method used to retrieve the ABL height was based on the detection of the drop off in the RSCS signals at the interface between the free troposphere and the ML.

The inflexion point method (IPM) was fit for determining ABL height using signals averaged over a period of time. The second-order derivative of averaged RSCS profiles with respect to the altitude was used to determine the absolute minimum value of the ABL. The height is thus defined as the middle of the transition zone (i.e., the interface between the ML and the free troposphere). This height definition slightly differs from the one associated with the first-order derivative approach that defines the height as the base of the transition zone (i.e., the top of the ML)[5]. However, limitations of the IPM are found in the presence of elevated humid aerosol-laden layers whenever the inversion capping of the mixed layer is weak. In this case, small aerosol gradients between the mixed layer and the free troposphere are much more difficult to detect than

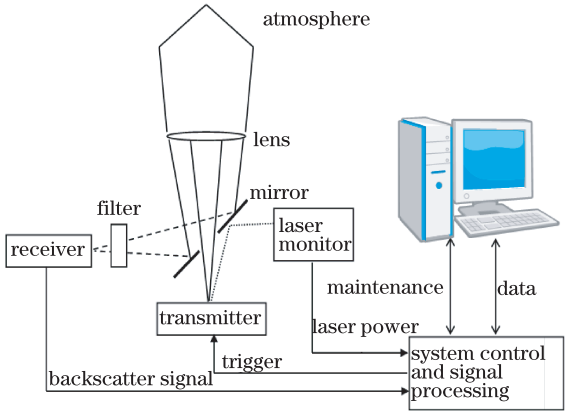

Fig. 1. Ceilometer system scheme.

Table 1. Ceilometer Vaisala CL31 Parameters

Beam Divergence	(±0.4 mrad) × (±0.7 mrad)
Field-of-View Divergence	0.83 mrad
Effective Lens Diameter	96 mm
Optics Focus Length	300 mm
Measurement Range	7500 m
Range Resolution	5 or 10 m
Report Interval	2–20 s
Laser Type	InGaAs Diode
Laser Wavelength	905 nm
Operating Mode	Pulsed
Pulse Properties	110 ns,1.2 μJ/pulse
Repetition Rate	10 kHz
Detector Type	Avalanche Photodiode
Receiver Bandwidth	30 MHz

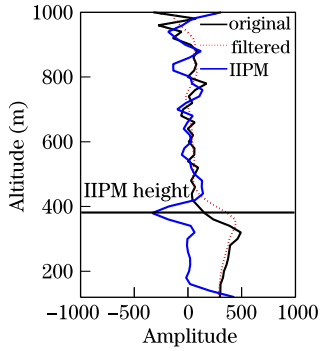

Fig. 2. Original backscatter, filtered, and IIPM profiles.

elevated layers that exhibit large aerosol and humidity gradients with respect to their surroundings[8]. This situation worsens when the background noise becomes stronger. The IIPM, presented in this letter, can relatively enhance the ability of detecting slow changes between MLs and the free troposphere by weakening other changes, especially background noise, as shown in Fig. 2. It has been proven that this method has the advantages of IPM and high accuracy.

This method of ABL height determination was tested using averaged lidar signals. The IIPM algorithm was

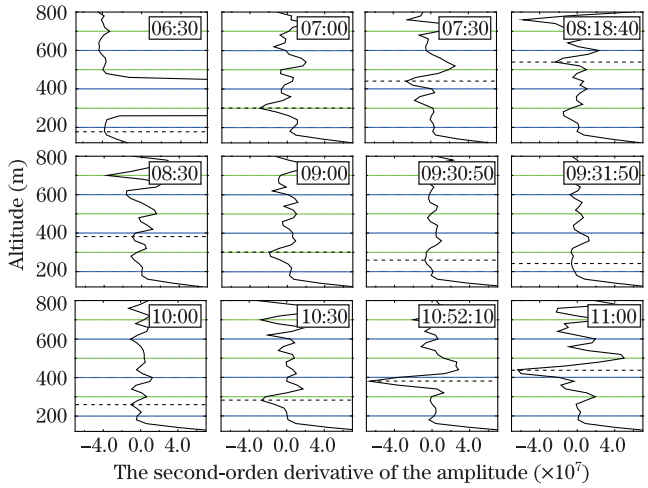

Fig. 3. Temporal evolution of the ABL observed using IIPM (dashed lines show ABL height).

designed to detect the second derivative peak, which has the minimum magnitude, similar to that of the IPM presented by Menut[8]. However, because of finite impulse response (FIR) filtering, the IIPM can achieve a more stable performance and have a lower failure rate than general IPM, as shown in Fig. 3.

With the objective of testing the IIPM and of investigating the evolution of ABL height due to the sudden attenuation of solar radiation, field experiments were conducted over Hefei City, which is right within the totality path of the solar eclipse on July 22, 2009. Hefei experienced 100% obscuration from 9:30:55 to 9:32:44 Beijing Time (BJT) during the solar eclipse. The partial eclipse took place from 8:18:40 to 10:52:09 BJT, with the maximum phase occurring at 9:31:47 BJT. It must be pointed out that clouds occasionally appeared during the eclipse, which might have affected our investigation.

The time series of averaged RSCS over Hefei for the total eclipse and the adjacent hours (from 00:00 to 23:59, July 22, 2009, BJT) are shown in Fig. 4. The intensity of the lidar backscatter signal is also shown at the right side of the figure. Although it is not precise, ABL development on the three-day observation period was easily recognized. At approximately 0:00 BJT, there was a brief shower. When it had cleared, ABL tended to be in a steady state, and its height exhibited a falling trend. After 3:00 BJT, the mist became denser and denser on the surface. Low clouds formed over Hefei at an altitude range of approximately 100–400 m, and remained until 07:30 BJT (see white spots among the dark ones in Fig. 4). In a sense, this inhibited aerosol lidar measurements. From 05:00 to 07:30 BJT, clouds and ABL height indicated a rising trend. At 07:00 BJT, ABL height was measured at approximately 450 m.

The backscatter profiles during the total eclipse showed noticeably higher signal-to-noise ratio (SNR) (caused by a reduced background noise) and more stable layer structures. At the early stages of the eclipse, radiative cooling began to take place near the surface, similar to the way the surface cools after sunset. At that time, due to turbulence mixing, the atmosphere was still mixed and temperature deficit extended from the surface at higher levels throughout the whole boundary layer, consequently decreasing ABL height. During the period encompassed by the beginning of the solar eclipse (08:18 BJT) and its maximum (09:31 BJT), ABL height decreased from 430 to 210 m. As an eclipse approaches its maximum phase, a pronounced temperature deficit is observed, and stable stratification is reached near the surface. Convectional mechanisms are expected to weaken and eventually break down as heat transfer is confined to a thinner layer above the ground. Owing to the stabilization of air at lower levels and the suppression of turbulent mechanisms, the conditions at higher levels remain relatively unchanged. This is also exhibited in Fig. 4, where the structure of the ABL is stable all the time from 09:20 to 10:10 BJT. As reported by Eaton *et al.,* during the maximum phase of an eclipse, the sensible heat and radiation fluxes are affected, turbulence is reduced, and the air refractive index structure constant is dramatically decreased[9,10] This resembles the phenomenon recorded during nighttime where the residual layer coexists with the nocturnal boundary layer.

Another important finding was the time lag of approximately 20 min for ABL structure and air temperature to respond to the eclipse, which supports Girard-Ardhuin's argument that an eclipse induces a clear response in the atmosphere with a time lag of 15 to 30 min. It is shown in Fig. 4 that the minimum ABL height (190 m) appeared at approximately 09:50 BJT, the trend of which was identical to that of the temperature. At about 09:50 BJT, ABL height again increased. From 09:50 to 10:30 BJT, when the eclipse was about to end, ABL height slowly and steadily increased up to 300 m as a result of the diminished but increasing irradiation of the Earth's sur-

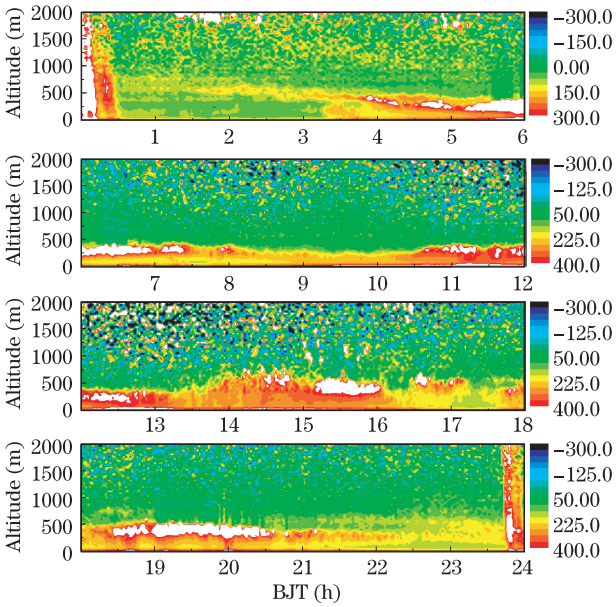

Fig. 4. Time-height cross-section of averaged RSCS over Hefei from 00:00 to 23:59 BJT, July 22, 2009.

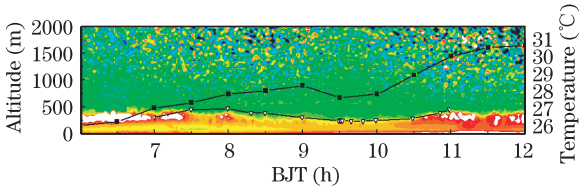

Fig. 5. ABL height (triangles) and temperature (dark squares) evolution over Hefei during the total eclipse.

face. After 10:30 BJT, ABL height increased more dramatically, reaching approximately 420 m at 11:00 BJT. Thereafter, it resumed an increasing trend to approximately 760 m. The maximum height for the whole day was observed at 14:45 BJT.

Figure 5 shows the time height cross section of the RSCS ceilometer signal during the total eclipse. The evolution of the ABL can be clearly seen. The triangles represent ABL heights calculated using the IIPM. Surface temperatures during the eclipse are shown as dark squares.

The IIPM presented in this letter can better assess the slow change between the ML and the free troposphere by weakening other changes, especially background noise. It has been proven that this method has the advantages of IPM and is highly accurate. The IIPM was used to investigate ABL evolution over Hefei before, during, and after the solar eclipse to document and analyze the dynamic and thermodynamic responses of the lower atmosphere to sudden changes in incoming solar radiation. As expected, the eclipse obviously affected ABL distribution. According to the observation, ABL height decreased from 430 m before the eclipse to 190 m after the total eclipse, and then increased to 750 m (14:45 BJT). The whole ABL changing process had a time lag of 20 min to respond to the eclipse.

This work was supported by the New Technology Research Foundation of the Chinese Meteorological Bureau under Grant No. GYHY200706023.

References

1. R. B. Stull, *An Introduction to Boundary Layer Meteorology* (Kluwer Academic Publishers, Dordrecht, 1988).
2. V. Amiridis, D. Melas, D. S. Balis, A. Papayannis, D. Founda, E. Katragkou, E. Giannakaki, R. E. Mamouri, E. Gerasopoulos, and C. Zerefos, Atmos. Chem. Phys. **7,** 6181 (2007).
3. Z. Chen, W. Liu, Y. Zhang, N. Zhao, J. He, and J. Ruan, Chin. Opt. Lett. **7,** 753 (2009).
4. S. Emeis, K. Schafer, and C. Munkel, Meteorologische Zeitschrift **17,** 621 (2008).
5. C. Flamant, J. Pelon, P. Flamant, and P. Durand, Boundary-Layer Meteorology **83,** 247 (1997).
6. H. Liu, Z. Ge, Z. Wang, W. Huang, and J. Zhou, Acta Opt. Sin. (in Chinese) **28,** 1837 (2008).
7. Y. Ma, H. Lin, H. Ji, and T. Dong, Chinese J. Lasers (in Chinese) **34,** 170 (2007).
8. L. Menut, C. Flamant, J. Pelon, and P. H. Flamant, Appl. Opt. **38,** 945 (1999).
9. F. D. Eaton, J. R. Hines, W. H. Hatch, R. M. Cionco, J. Byers, D. Garvey, and D. R. Miller, Boundary-Layer Meteorology **83,** 331 (1997).
10. P. Zanis, E. Katragkou, M. Kanakidou, B. E. Psiloglou, S. Karathanasis, M. Vrekoussis, E. Gerasopoulos, I. Lisaridis, K. Markakis, A. Poupkou, V. Amiridis, D. Melas, N. Mihalopoulos, and C. Zerefos, Atmos. Chem. Phys. **7,** 6061 (2007).